Optimization of isopropyl alcohol degradation by microwave-induced catalytic oxidation process

Quynh Thi Phuong Tran, Chi-Hsu Hsieh, Tung-Yu Yang and Hsin-hsin Tung

ABSTRACT

Isopropyl alcohol (IPA) is a common waste solvent from the semiconductor and optoelectronic manufacturing industries. The current study assesses the feasibility of microwave-induced catalytic oxidation process for synthetic IPA wastewater. The effect of three independent variables, including oxidant (hydrogen peroxide), initial IPA concentration, and dosage of catalyst (granular activated carbon, GAC) on the IPA removal efficiency, were investigated and optimized by response surface methodology based on central composite design. The estimated optimal working conditions were as follows: $[H_2O_2] < 0.132$ M, GAC dosage = 108–123 g/L, and initial $[IPA] = 0.038–0.10$ M. The findings indicated that the dosage of GAC and the initial IPA concentration strongly affected the overall IPA removal. The values of $R^2 = 0.9948$ and adjusted $R^2 = 0.9901$ demonstrated that the response variability could be explained by the model expressing a satisfactory quadratic fit. Finally, the $H_2O_2/GAC/MW$ process showed a faster and higher IPA removal rate than other processes tested.

Key words | central composite design, isopropyl alcohol, microwave-induced catalytic oxidation, response surface methodology

Quynh Thi Phuong Tran
Hsin-hsin Tung (corresponding author)
Graduate Institute of Environmental Engineering,
National Taiwan University,
1 Sec4 Roosevelt Rd, Taipei 10617,
Taiwan
E-mail: htung@ntu.edu.tw

Chi-Hsu Hsieh
Tung-Yu Yang
Topco Scientific Co. Ltd,
No. 483, Sec. 2, Tiding Blvd, Neihu, Taipei City
11493,
Taiwan

INTRODUCTION

Isopropyl alcohol (IPA) (C_3H_8O) – a colorless, flammable compound with a strong odor – is an important solvent widely used as a cleaning agent in the electronic and precision machinery industries. In the typical semiconductor manufacturing processes, a large amount of high-purity IPA is consumed and discharged as waste solvent after wafer surface washing and cleaning (Kuila & Ray 2013). IPA and its metabolite, acetone (C_3H_6O), are considered as hazardous and toxic water wastes (B3) (Abdulloh *et al.* 2019) that act as depressants of the human central nervous system, causing unconsciousness and ending in a deep coma (Ashurst & Nappe 2019; Sivilotti 2019).

Traditional methods involving physicochemical decomposition or microorganisms have shown limited efficiencies for treating IPA-containing wastewater (Cheng *et al.* 2010). The high concentration of IPA can be separated from the waste solvent by pervaporation using copolymer membrane (acrylonitrile and methyl acrylate) (Kuila & Ray 2013). However, the pervaporation process is complex and not easy to operate. An integrated method consisting of air stripping and activated carbon fiber columns is employed to recover IPA in waste (Lin & Wang 2004). It is relatively easy, but requires pH control and cannot be carried out at low temperatures (Abdulloh *et al.* 2019). In a previous study, Xiao *et al.* (2015) reported that both sequencing batch biofilm reactor (SBBR) and sequencing batch reactor (SBR) are effective for removing IPA. Nevertheless, the biofilm will be damaged as the chemical oxygen demand is higher than 1,600 mg/L.

In recent years, the microwave-induced catalytic oxidation process has been widely proposed in the literature as an attractive alternative technique. This process shortens reaction time, reduces equipment size, provides greater ease of operation, and increases treatment performance (Xu et al. 2014; Liu et al. 2018). In fact, its efficiency strongly depends on numerous process parameters (Bi et al. 2007; Liu et al. 2014) such as the characteristics of the catalyst, dosage of catalyst, oxidant concentration, and initial pollutants concentration.
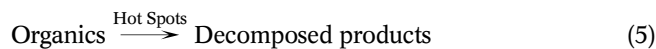
First, it is well known that the catalyst plays an important role in the microwave-induced catalytic oxidation process (Quan et al. 2007; Liu et al. 2018). It has to be a microwave-absorbing material capable of both producing large amounts of surface 'hot spots' – where more rapid oxidation occurs – and generating great amounts of •OH catalyzed, leading to a significant degradation rate in a shorter irradiation time (Remya & Lin 2011; Yin et al. 2016).

Besides this, another apparent characteristic for the catalyst in the oxidation process can be surface area and pore structure. Specifically, the large surface area and porosity in the catalyst are able to provide many active sites to trigger the chemical reaction of oxidation of organic pollutants (Chen & Shen 2016). Several catalysts such as copper oxides (Atta et al. 2012; Liu et al. 2018), zero-valence iron (Jou 2008; Lee et al. 2012), nickel oxides (Lai et al. 2006), activated carbon (AC) (Quan et al. 2007) or AC supported metal (Liu et al. 2018) have been investigated to enhance organic compounds' removal in microwave-induced catalytic oxidation process. Among all, AC can be a promising catalyst for IPA degradation owing to the huge surface area (994.145 m^2/g), the developed pore structure (0.526 cm^3/g), and the excellent capability for microwave (MW) energy absorption (Quan et al. 2007).

Furthermore, the amount of catalyst is a crucial factor that influences the microwave-induced catalytic oxidation process. Several studies have reported that increasing the dosage of catalyst increases the rate of degradation continuously (Zhang et al. 2012; Singh et al. 2013; Yang et al. 2013) as a result of the presence of a higher number of activated absorbed photons and available sites.

The dosage of oxidants is also well known as one of the variables influencing pollutant removal performance. Liu et al. (2018) indicated that the degradation rate of phenol increased nonlinearly with an increase in the concentration of H_2O_2.

The initial concentration of pollutants is another parameter affecting the rates of degradation. Literature revealed that the degradation rate of organic pollutants decreased with increasing initial pollutants' concentration (Bi et al. 2007; Prasannakumar Beri et al. 2008; Mohanraj et al. 2015).

$$H_2O_2 \xrightarrow{\text{MW}} 2OH^\bullet \tag{1}$$

$$\text{Solid catalyst} \xrightarrow{\text{MW}} OH^\bullet \tag{2}$$

$$OH^\bullet + \text{Organics} \rightarrow \text{Decomposed products} \tag{3}$$

$$\text{Solid catalyst} \xrightarrow{\text{MW}} \text{'Hot spots'} \tag{4}$$

$$\text{Organics} \xrightarrow{\text{Hot Spots}} \text{Decomposed products} \tag{5}$$

To the best of our knowledge, the details of treating IPA wastewater by the MW-induced catalytic oxidation process were unclear in the literature, as well as the optimum operating conditions. Due to the synergistic effects between different variables, the application of the conventional methods for process optimization would require a large number of experiments, times, and materials. To overcome these drawbacks, optimizing the experimental conditions with a statistical design tool becomes extremely necessary. Among statistical tools used in environmental health engineering, response surface methodology (RSM) has already proven to be a reliable statistical tool for evaluating the effects of independent variables on response performance and for predicting the best degree of response (Mohammadi et al. 2017).

Considering the above-mentioned facts, the current research aimed to optimize the operating factors – initial IPA concentration and dosage of granular activated carbon (GAC) and hydrogen peroxide – in the microwave-induced catalytic oxidation process using a central composite design (CCD) combined with RSM, as well as to assess the influence of MW on the degradation of IPA-containing wastewater.

MATERIALS AND METHODS

Chemicals and materials

Isopropyl alcohol 99.5% ($CH_3CHOHCH_3$) was purchased from J.T. Baker. Analytical-reagent grade hydrogen peroxide (H_2O_2) and ortho-phosphoric acid 85% (H_3PO_4) were

Table 1 │ Characteristics of granular activated carbon

Parameter	Granular activated carbon (GAC)
Shape	Sphere
Particle size (mm)	0.35–0.8
Bulk density (g/mL)	Approx. 0.6
Specific surface area (m^2/g)	994.145
Pore volume (cm^3/g)	0.526
Average pore diameter (nm)	2.117
Iodine absorption capacity (mg/g)	1,200–1,350
Residue on ignition (ash)	0.05% or less

purchased from Sigma-Aldrich. Ultra-pure deionized water of 18.2 MΩ·cm resistivity was obtained from Milli-Q® Integral ultrapure water apparatus and used throughout the total organic carbon (TOC) analysis experiment. Granular activated carbon (GAC, Kureha Trading Co., Ltd, Japan), with a mean diameter of 0.58 mm, was applied as the solid catalyst in this study. Table 1 lists the physical properties of GAC used in this study. Before use, the virgin GAC was dried in an oven at 150 °C for 24 h and then cooled to ambient temperature in a desiccator. All other reagents used in this study were of the highest grade available.

Experimental procedure and analytical methods

Figure 1 is a schematic diagram for the laboratory setup. A microwave digestion laboratory station (Milestone, Ethos Plus 1, frequency 2,450 MHz, max power 1,500 W) was used for generating the microwave energy. In a standard reaction run, 10 mL of IPA solution (0.038–0.743 M) was transferred to a 100 mL Teflon vessel. The desired volume of hydrogen peroxide solution (30% in weight) was injected into the vessel under stirring. Then, a measured amount of GAC catalyst was added to this IPA solution and irradiated for 120 seconds in the microwave digestion laboratory station. The solution temperature was kept at 80 ± 2 °C and MW power at 600 W throughout all of the experiments. At the end of each run, the remaining IPA was determined as the TOC in the samples (Aurora 1030 W TOC Analyzer, O.I. Analytical Corporation). The amount of TOC removed from the synthetic IPA samples in the microwave-induced catalytic oxidation process was calculated using Equation (6):

$$\text{TOC removal efficiency (\%)} = \frac{C_0 - C}{C_0} \times 100 \qquad (6)$$

where C_0 and C represent the initial and effluent concentration of TOC (mg/L) respectively.

The Brunauer–Emmett–Teller (BET) surface area of the solid catalysts was characterized by nitrogen adsorption/desorption isotherms on a Micromeritics ASAP 2020 Surface Area and Porosity Analyzer Software V3.00. Typically, 0.2–0.3 g of the sample was used for the measurement and the samples were previously outgassed for at least 8 h at 150 °C prior to N$_2$ adsorption.
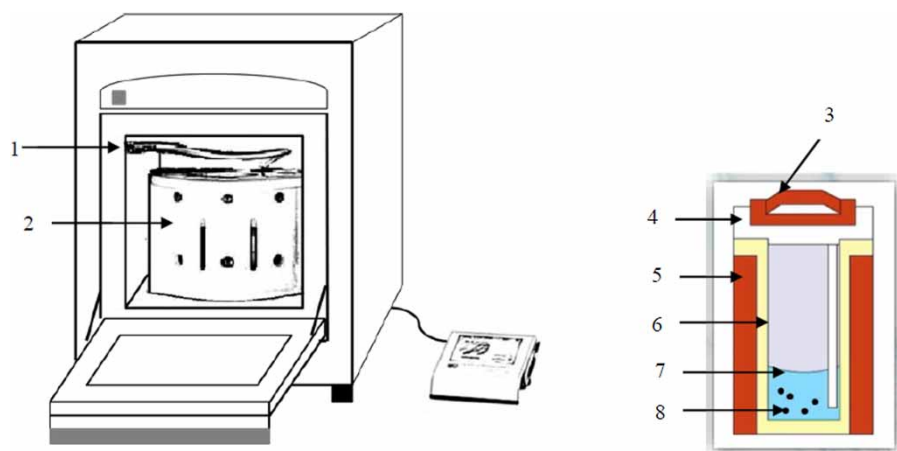

Figure 1 │ Schematic diagram of microwave reactor system. (1) Direct sensor for temperature and pressure control, (2) high pressure rotor, (3) safety spring and adapter plate, (4) cover, (5) safety shield, (6) vessel, (7) IPA and oxidant, and (8) solid catalyst (Hamid 2015).

Central composite design

The essence of any process relies on the level of the design at which the response reaches the optimum. A variety of techniques available have been applied to the design of experiments, however, the RSM outperforms other techniques due to its simplicity (Haque *et al.* 2016; Bharath *et al.* 2019; Basheer *et al.* 2019). The RSM is a combination of statistical and mathematical methods used to develop, improve, and optimize the processes (Arslan-Alaton *et al.* 2009; Montgomery 2014; Behera *et al.* 2018). A reduction in the number of experiments and investigation of the effects of interactions between variables are among the advantages of RSM (Parolin *et al.* 2013; Sarrai *et al.* 2016; Mohammadi *et al.* 2017).

In this study, a CCD with three independent variables was used to assess the influences of H_2O_2, GAC dosage, and initial IPA concentration on the TOC removal efficiency under the microwave-induced catalytic oxidation process. In addition, the interactions between the selected variables were also determined by using RSM. A total of 20 experiments were selected to determine the coefficients of the second-order polynomial regression model for three variables. Each variable was studied at five levels (± 1 for the factorial points, 0 for the center points, and ± 1.682 for the axial points), as presented in Table 2. The behavior of the microwave-induced catalytic oxidation process is explained by the following empirical second-order polynomial model (Equation (7)) (Younis *et al.* 2014; Sarrai *et al.* 2016):

$$Y\% = \alpha_0 + \sum_{i=1}^{k} \alpha_i X_i + \sum_{i=1}^{k} \alpha_{ii} X_i^2 + \sum_{i=j}^{k-1} \sum_{i=j+1}^{k} \alpha_{ij} X_i X_j \tag{7}$$

where Y is the predicted response (TOC degradation by the microwave-induced catalytic oxidation); α_0 and α_i are the constant coefficient and linear coefficient, respectively; α_{ii} and α_{ij}

are the quadratic coefficients and interaction coefficients, respectively; and X_i and X_j are coded values of the independent process factors which refer to the factors i and j, respectively.

RESULTS AND DISCUSSION

RSM model construction

Table 3 displays the observed and predicted results for the percent of TOC removal. The R software was used to estimate the coefficients of the second-order fitting equation, as well as to test the suitability of the model. As a result, the second-order polynomial equation was given as follows:

$$\begin{aligned} Y\% = {} & 44.213 - 62.407X_1 + 0.821X_2 - 62.001X_3 \\ & + 0.011X_1X_2 - 3.810X_1X_3 - 0.203X_2X_3 \\ & + 74.439X_1^2 - 0.002X_2^2 + 39.495X_3^2 \end{aligned} \tag{8}$$

The model adequacy check is an integral part of the data analysis procedure (Ivanescu *et al.* 2016), and the approximating model would give poor or misleading results if the fit is inadequate (Körbahti 2007). Specifically, the coefficient of determination (R^2) and the adjusted coefficient of determination (R^2_{adjust}) was used to describe the fit quality of the polynomial model, and Fisher's *F*-test and the probability value $> F$ was used to check the statistical significance. Table 4 summarizes the analysis-of-variance (ANOVA) results of the response surface quadratic model for TOC removal by the microwave-induced catalytic oxidation process. The mean squares were determined by dividing the sum of squares of each variation by the respective degrees of freedom (DF). The model *F*-value was calculated by dividing the model mean square by the residual mean square. In addition, a 95% confidence level (significance level $\alpha = 0.05$) was chosen to evaluate the statistical significance.

The large value of *R*-squared for Equation (8) indicates that 99.48% of the total variations could be satisfactorily explained by the second-order polynomial regression model. As well, the small probability values (*p*-value <0.001) for all regressions are given in Table 4. This denotes that the established model is highly significant for the TOC removal response.

Table 2 | Experimental range and levels of independent variables

| Independent variables | Code | Real values of the coded levels | | | | |
		−1.682	−1	0	+1	+1.682
Concentration of H_2O_2 (M)	X_1	0.132	0.2	0.3	0.4	0.468
Dosage of GAC (g/L)	X_2	39.54	60	90	120	140.46
Concentration of IPA (M)	X_3	0.038	0.18	0.39	0.60	0.743

Table 3 | Design matrix by CCD, and the actual and predicted percentage TOC degradation for response surface quadratic model

Run number	Coded levels			Actual levels			TOC removal (%)	
	X_1	X_2	X_3	$[H_2O_2]_0$ (M)	GAC dosage (g/L)	$[IPA]_0$ (M)	Observed	Predicted
1	−1	−1	−1	0.2	60	0.18	63.18	64.69
2	+1	−1	−1	0.4	60	0.18	58.74	61.14
3	−1	+1	−1	0.2	120	0.18	84.83	90.29
4	−1	−1	+1	0.2	60	0.60	45.69	46.15
5	+1	+1	−1	0.4	120	0.18	81.16	86.87
6	+1	−1	+1	0.4	60	0.60	41.57	42.28
7	−1	+1	+1	0.2	120	0.60	62.87	66.64
8	+1	+1	+1	0.4	120	0.60	58.24	62.90
9	−1.682	0	0	0.132	90	0.39	65.34	69.60
10	+1.682	0	0	0.468	90	0.39	60.55	63.47
11	0	−1.682	0	0.3	39.54	0.39	39.39	39.91
12	0	+1.682	0	0.3	140.46	0.39	70.18	78.77
13	0	0	−1.682	0.3	90	0.038	85.17	87.14
14	0	0	+1.682	0.3	90	0.743	46.29	51.49
15	0	0	0	0.3	90	0.39	61.54	64.43
16	0	0	0	0.3	90	0.39	60.89	64.43
17	0	0	0	0.3	90	0.39	61.34	64.43
18	0	0	0	0.3	90	0.39	61.58	64.43
19	0	0	0	0.3	90	0.39	62.11	64.43
20	0	0	0	0.3	90	0.39	60.75	64.43

Influences of the selected variables and their interactions

In this study, the probability value $>|t|$ or p-value or asymptotic significance was used in the context of the null hypothesis testing in order to quantify the idea of the statistical significance of each independent variable. If the probability value is less than the chosen significance level (α), that suggests that the null hypothesis may be rejected and the curvature is not significant. To be more specific, traditionally, 5% was used as the significance level of the test, and the null hypothesis is rejected when the p-value is less

Table 4 | ANOVA results of the response surface quadratic model for TOC removal by the microwave-induced catalytic oxidation process

Source	Degrees of freedom	Sum of squares	Mean square	F value	Pr (>F)	Remark
Model[a]						
FO (X_1, X_2, X_3)	3	2,814.63	938.21	603.4079	1.352×10^{-11}	Highly significant
TWI (X_1, X_2, X_3)	3	13.12	4.37	2.8118	0.093891	Significant
PQ (X_1, X_2, X_3)	3	130.31	43.44	27.9371	3.556×10^{-5}	Highly significant
Residuals	10	15.55	1.55	–	–	–
Lack of fit	5	14.31	2.86	11.5768	0.008872	Significant
Pure error	5	1.24	0.25	–	–	–

[a]FO, TWI, and PQ represent first-order, two-way interaction, and pure quadratic, respectively.

Table 5 │ Statistical analysis of the individual terms present in the model equation

Term	Coefficient	Standard error	t value	Pr (>| t |)	Remark
α_0	44.213	6.9690	6.3442	8.414×10^{-5}	Highly significant
α_1	−62.407	25.3580	−2.4611	0.033615	Significant
α_2	0.821	0.0844	9.7222	2.057×10^{-6}	Highly significant
α_3	−62.001	10.7660	−5.7587	0.000183	Highly significant
α_{12}	0.011	0.1470	0.0737	0.942687	Not significant
α_{13}	−3.810	20.9930	−0.1815	0.859629	Not significant
α_{23}	−0.203	0.0700	−2.8978	0.015895	Significant
α_{11}	74.439	32.9000	2.2626	0.047158	Significant
α_{22}	−0.002	0.0004	−6.5235	6.693×10^{-5}	Highly significant
α_{33}	39.495	7.4705	5.2868	0.000354	Highly significant
Multiple R-squared: 0.9948			Adjusted R-squared: 0.9901		

than 0.05 and not rejected when the value is greater than 0.05 (Wikipedia). As depicted in Table 5, the p-value <0.001 means that the independent variables of the quadratic model are considered highly statistically significant which includes the interception coefficient, the dosage of GAC (X_2), the initial concentration of IPA (X_3), the second-order effect of GAC dosage (X_2^2), and the second-order effect of the initial IPA concentration (X_3^2). Additionally, the concentration of H_2O_2 (X_1), the interaction between the GAC dosage and the initial IPA concentration (X_{23}), and the second-order effect of H_2O_2 concentration (X_1^2) are statistically significant since p-value <0.05. Nevertheless, when the p-value is larger than 0.05, the interaction between the H_2O_2 concentration and the GAC dosage (X_{12}), as well as the interaction between the initial IPA concentration and the H_2O_2 concentration (X_{13}), are insignificant. According to the regression model, the order of priority among the main effect of the selected variables is the dosage of GAC (X_2) > the initial IPA concentration (X_3) > the H_2O_2 concentration (X_1).

The two-dimensional diagrams of the model-predicted responses – while one variable was kept at the constant and the others were varied within the experimental ranges – were obtained by R software. The results from these diagrams were utilized to assess the interactive effects of the independent variables and the percentage of TOC removal in the microwave-induced catalytic oxidation process.

Influence of hydrogen peroxide and initial IPA concentration on TOC removal

Percent TOC removal efficiencies as a function of H_2O_2 concentration and initial IPA concentration are illustrated in Figure 2. As can be seen in the response contour, increasing the initial IPA concentration from 0.038 to 0.743 M led to a dramatic decrease in the TOC removal rate from 85.17 to 46.29%. It is possibly because the number of electron-hole pairs and free radicals (OH•) is kept constant under the same applied reaction condition, while the initial IPA concentration is increased (Regulska *et al.* 2016). In other words, a comparatively less amount of oxidizing groups is available for attacking the IPA molecules. Similarly, the TOC degradation performance also decreased gradually
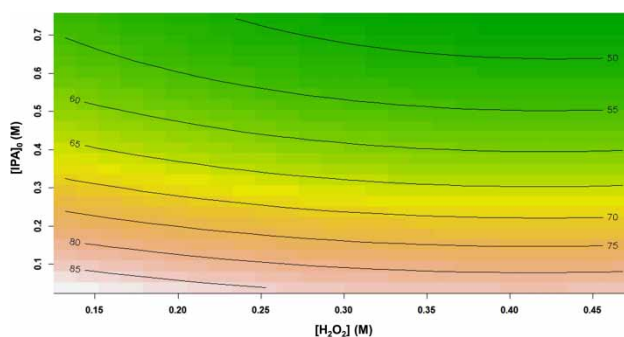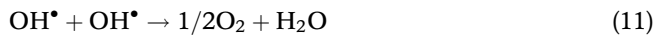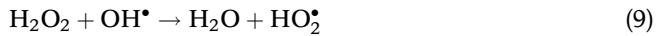

Figure 2 │ Interaction effects of H_2O_2 concentration and initial IPA concentration, and their influences on TOC removal rate. The dosage of GAC was kept constant at 90 g/L.

with an increase in H_2O_2 concentration. An excess H_2O_2 may promote the occurrence of auto-scavenging reactions as follows (Bautista et al. 2007; Iboukhoulef et al. 2013; Zhang & Li 2014):

$$H_2O_2 + OH^\bullet \rightarrow H_2O + HO_2^\bullet \tag{9}$$

$$HO_2^\bullet + OH^\bullet \rightarrow O_2 + H_2O \tag{10}$$

$$OH^\bullet + OH^\bullet \rightarrow 1/2O_2 + H_2O \tag{11}$$

Another radical ($HO_2^\bullet$) will be formed with an oxidation potential considerably smaller than $OH^\bullet$. It competes for $OH^\bullet$ to inhibit oxidation of the target organic pollutant, which reduces the probability of the attacking OH on the organic molecule (Iboukhoulef et al. 2013; Zhang & Li 2014; Liu et al. 2018). The contour plots indicate that the optimum region for the efficient TOC removal is in the initial IPA concentration range of 0.038 to 0.10 M. Unfortunately, the optimum level of H_2O_2 has not been pointed out in this study. However, it can be concluded that the concentration of H_2O_2 should be lower than 0.132 M.

Influence of GAC dosage and initial IPA concentration on TOC removal

Figure 3 demonstrates the interaction effect of GAC dosage and the initial IPA concentration on the TOC removal efficiency. It can be clearly observed that at the initial IPA concentration of 0.1 M, an increase of the GAC dosage from 40 to 140 g/L significantly raised TOC removal
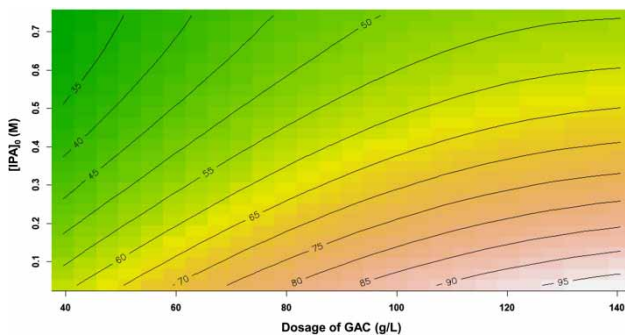
efficiency from 55 to 92%. The greater the catalyst dosage, the greater the number of hydroxyl radicals and hot spots generated, resulting in a higher degradation rate of TOC (Gao et al. 2016). The result is consistent with other research that the catalyst acts in an important role in the microwave-induced catalytic oxidation process (Liu et al. 2018). It can be concluded from the contour plots that the catalyst dosage range of 108 to 123 g/L is the optimum region for TOC removal rate.

Influence of hydrogen peroxide concentration and GAC dosage on TOC removal

Figure 4 describes the interaction effect of H_2O_2 concentration and GAC dosage on the TOC removal efficiency. As illustrated in the response contour, the TOC degradation performance is greater than 67% in the catalyst dosage range of 97 to 120 g/L at either low or high concentration of H_2O_2. Consequently, it is noticeable that there is a slight decrease in the TOC removal efficiency with the increase of H_2O_2 concentration. Increasing H_2O_2 concentration probably created the inhibitory (hydroxyl radicals scavenging) effect resulting in the generation of $HO_2^\bullet$ with lower oxidation potential. Additionally, it also can be observed in Figure 4 that increasing the GAC dosage had a positive effect on TOC removal at all selected initial H_2O_2 concentration. Hydrogen peroxide can be activated on the carbon surface involving the formation of reactive free radicals that are able to oxidize IPA. The more GAC was used, the more hydroxyl radicals were produced. This assists in the higher degradation rate of IPA.
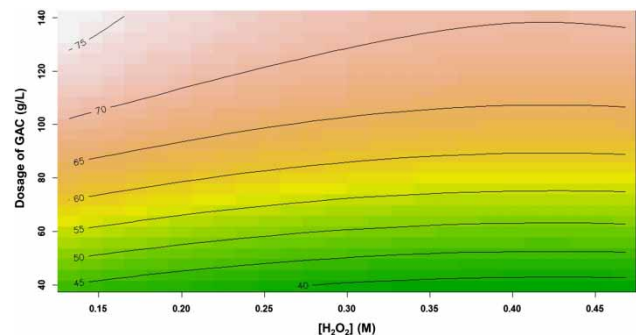

Figure 3 │ Interaction effects of GAC dosage and initial concentration of IPA, and their influences on TOC removal rate. The concentration of H_2O_2 was kept constant at 0.3 M.

Figure 4 │ Interaction effects of H_2O_2 concentration and GAC dosage, and their influences on TOC removal rate. Initial concentration of IPA was kept constant at 0.39 M.

Table 6 │ Comparison of the model-predicted and experimental results under the optimized working conditions

	Experimental parameters			TOC removal efficiency (%)	
	H_2O_2 concentration (X_1, M)	GAC dosage (X_2, g/L)	Initial IPA concentration (X_3, M)	Predicted	Experimental
Optimum working conditions	0.132	108	0.038	99.62	90.5
	0.132	115	0.070	99.59	89.9
	0.132	123	0.100	99.82	90.7

Optimization of microwave-induced catalytic oxidation treatment of IPA-containing wastewater

The new experiments were run under optimized working conditions to confirm the validity of the empirical second-order polynomial model. As aforementioned, the optimum values were established as $H_2O_2 = 0.132$ M, GAC = 108–123 g/L, and IPA = 0.038–0.10 M to achieve the maximum removal of TOC. The experimental results in Table 6 are rather close to those obtained using response surface analysis, implying that RSM could be used effectively to optimize process parameters in a complex process using the statistical design of experiments. The findings are remarkably similar to previous study results (Prasannakumar Beri et al. 2008; Arslan-Alaton et al. 2009; Parolin et al. 2013; Sarrai et al. 2016; Mohammadi et al. 2017).

Comparison of different treatment processes on TOC removal

The effects of MW-induced irradiation were assessed by comparing the TOC removal rates in different treatment processes (H_2O_2, GAC, H_2O_2/GAC, H_2O_2/MW, GAC/MW, and H_2O_2/GAC/MW). It can be observed in Figure 5 that the TOC cannot be efficiently removed in short reaction time (2 min) by H_2O_2 alone, GAC adsorption, as well as combined H_2O_2 and GAC, in which the degradation efficiencies are all less than 20%. Nonetheless, MW irradiation did improve the usage efficiency of H_2O_2 and GAC by the generation of free radicals and 'hot spots' that is useful to achieve faster degradation in a shorter period of time. Specifically, H_2O_2 on its own exhibited low TOC removal efficiency rates, when combined with MW irradiation the removal efficiency jumped to 33.5%. It is possible that the
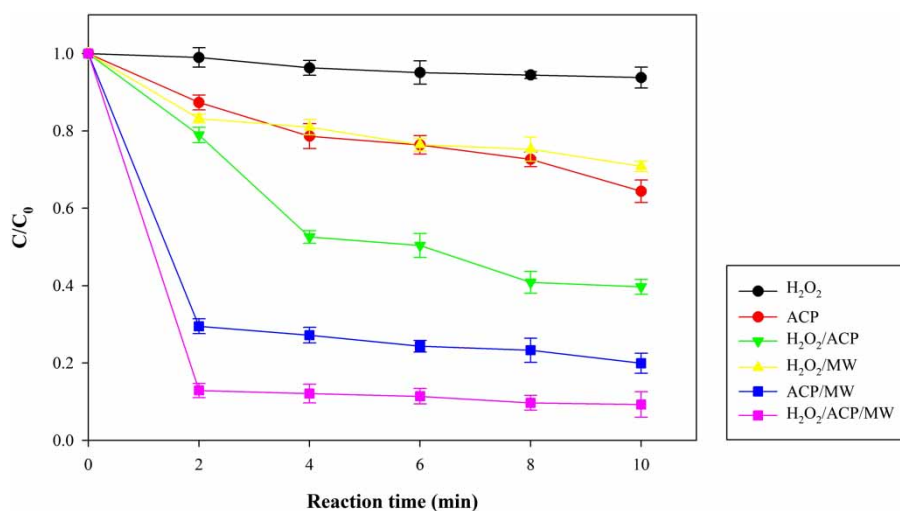
Figure 5 │ TOC removal by different treatment processes. Operational conditions: $[IPA]_0 = 0.038$ M, $[H_2O_2] = 0.132$ M, $Q_{catalyst} = 108$ g/L, $P_{MW} = 600$ W, irradiation time = 0–10 min, and reaction temperature = 80 °C.

elevated temperature did increase the decomposition of H_2O_2 into $^\bullet OH$ radicals (Equation (1)) and therefore enhanced the oxidation process when both H_2O_2 and MW were applied simultaneously. This result is consistent with the findings of Eskicioglu et al. (2008). As expected, increasing significantly the 'hot spots' on the surface of GAC led to a dramatic increase in percent TOC removals from 13.2% to 70.2%. Remya & Lin (2011) pointed out that the hot-spot formation on the surface of the catalyst is mainly responsible for the rapid degradation of pollutants adsorbed near the 'hot spots'. In addition, the coupling of MW to MW-absorbing materials acts sequentially and simultaneously in two ways for pollutant removal, i.e., (i) as adsorbent and (ii) as MW-absorbent. Furthermore, the TOC degradation efficiency of GAC/MW process went up from 70.2% to 88.7% with the addition of H_2O_2. It indicated that MW irradiation combined with the catalyst can promote the H_2O_2 decomposition to generate more $^\bullet OH$, thereby enhancing the degradation of the residual organic contaminant. Liu et al. (2018) also demonstrated that the effect of the simultaneous combination of H_2O_2 catalytic oxidation and MW irradiation can be responsible for the significant increase of the removal percentage of several pollutants in aqueous solution. Therefore, it can be concluded that an active catalyst, H_2O_2, and MW irradiation are extremely necessary for the effective treatment of TOC from the synthetic IPA aqueous solution in the microwave-induced catalytic oxidation process.

The mechanism of IPA degradation in the MW-induced catalytic oxidation process is proposed in Figure 6. Under the microwave irradiation, the GAC could strongly adsorb microwave energies, followed by the formation of numerous 'hot spots' on the surface of GAC. To be more specific, the kinetic energy of the π-electrons on the surface of the GAC is increased during the MW irradiation, which enables them to jump out of the material leading to the formation of 'hot spots' by ionizing the surrounding atmosphere (Menéndez et al. 2010; Remya & Lin 2011). The temperature of these 'hot spots' can ordinarily reach 1,200 °C (Zhang et al. 2007), resulting in the selective heating, molecular rotation, and final decrease of the activation energy of the chemical reaction (Zhang et al. 2013). Thus, the IPA adsorbed near the micro-'hot spots' on the GAC surface can be rapidly decomposed in the presence of oxygen (O_2) dissolved in water. The current research results are similar to some previous study findings (Polaert et al. 2005; Zhang et al. 2007). However, Liu et al. (2018) have reported that the degradation efficiency of adsorbed phenol resulting from 'hot spots' is limited. This was possibly due to the low specific surface area of the catalyst leading to less 'hot spots' and also due to the low concentration of phenol adsorbed by the catalyst resulting in less degradation efficiency caused by the 'hot spots'. Also, in this case, there is still approximately 30% of the residual organic contaminant in the aqueous solution that is difficult to be degraded since it cannot be adsorbed on activated carbon. Further addition of H_2O_2 allowed more than 90% elimination of TOC from the synthetic IPA aqueous solution. The dipolar polarization mechanism creates the elevated temperature within a short span, which provokes the increased decomposition of
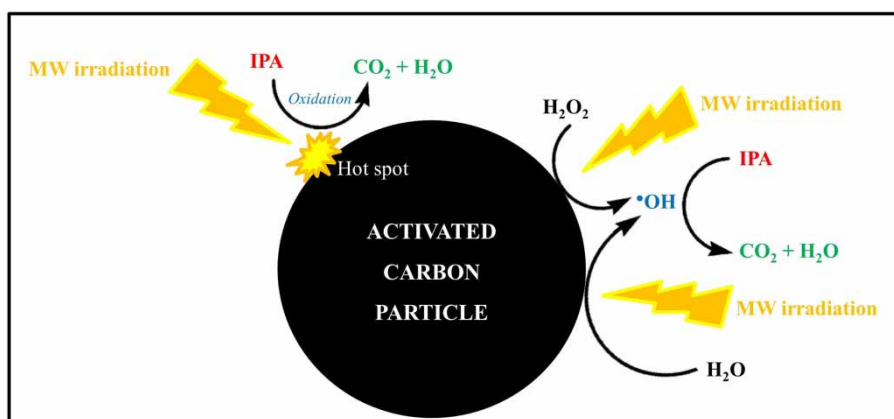

Figure 6 | A proposed mechanism of IPA degradation in H_2O_2/GAC/MW combined process.

H_2O_2 into $^\bullet OH$ (Remya & Lin 2011). The hydroxyl radicals have a strong capacity to oxidize IPA into CO_2 and H_2O.

CONCLUSIONS

In the current study, the effect of hydrogen peroxide, initial IPA concentration, and dosage of a solid catalyst on the TOC removal efficiency was investigated and optimized by using the RSM based on CCD. The combination of them supplied a powerful tool in the optimization of the microwave-induced catalytic oxidation process. In addition, the influence of microwaves (MW) on the TOC degradation from the synthetic IPA aqueous solution was evaluated. It was found that the TOC removal rate increased as the dosage of catalyst increased and the initial IPA concentration decreased. On the other hand, the TOC removal efficiency went down gradually with an increase of the H_2O_2 concentration. The estimated optimal conditions were as follows: $[H_2O_2]$ <0.132 M, GAC dosage = 108–123 g/L, and initial $[IPA]$ = 0.038–0.10 M. A TOC degradation of approximately 90% was achieved under the optimized working conditions, giving a high validity of the model. Finally, the H_2O_2/GAC/MW process had a shorter reaction time and a higher removal rate than other tested processes, possibly owing to synergistic effects of H_2O_2 with the catalyst and MW irradiation.

ACKNOWLEDGEMENTS

REFERENCES

Abdulloh, A., Supriyanto, G. & W Ningsih, O. 2019 Adsorption of Isopropyl Alcohol (IPA) in Water Using Activated Bentonite. In: *IOP Conference Series: Earth and Environmental Science*, Vol. 217, No. 1.

Arslan-Alaton, I., Tureli, G. & Olmez-Hanci, T. 2009 Treatment of azo dye production wastewaters using Photo-Fenton-like advanced oxidation processes: optimization by response surface methodology. *Journal of Photochemistry and Photobiology A: Chemistry* **202** (2), 142–153.

Ashurst, J. V. & Nappe, T. M. 2019 *Isopropanol Toxicity*. StatPeals Pubishing LLC, Treasure Island, FL. https://www.ncbi.nlm. nih.gov/books/NBK493181.

Atta, A. Y., Jibril, B. Y., Al-Waheibi, T. K. & Al-Waheibi, Y. M. 2012 Microwave-enhanced catalytic degradation of 2-nitrophenol on alumina-supported copper oxides. *Catalysis Communications* **26**, 112–116.

Basheer, O., Hanafiah, A. M., Abdulhakim Alsaadi, M. A., Al-Douri, Y., Malek, M. A., Mohammed Aljumaily, M. & Saadi Fiyadh, S. 2019 Synthesis and characterization of natural extracted precursor date palm fibre-based activated carbon for aluminum removal by RSM optimization. *Processes* **7** (5), 249.

Bautista, P., Mohedano, A. F., Gilarranz, M. A., Casas, J. A. & Rodriguez, J. J. 2007 Application of Fenton oxidation to cosmetic wastewaters treatment. *Journal of Hazardous Materials* **143** (1), 128–134.

Behera, S. K., Meena, H., Chakraborty, S. & Meikap, B. C. 2018 Application of response surface methodology (RSM) for optimization of leaching parameters for ash reduction from low-grade coal. *International Journal of Mining Science and Technology* **28** (4), 621–629.

Bharath, K. N., Manjunatha, G. B. & Santhosh, K. 2019 Failure analysis and the optimal and the toughness design of sheep-wool reinforced epoxy composites. In: *Failure Analysis in Biocomposites, Fibre-Reinforced Composites and Hybrid Composites* (M. Jawaid, M. Thariq & N. Saba, eds). Woodhead Publishing, Duxford, UK, pp. 97–107.

Bi, X.-y., Wang, P., Jiang, H., Xu, H.-y., Shi, S.-j. & Huang, J.-l. 2007 Treatment of phenol wastewater by microwave-induced ClO_2-CuO_x/Al_2O_3 catalytic oxidation process. *Journal of Environmental Sciences* **19** (12), 1510–1515.

Chen, W.-H. & Shen, C.-T. 2016 Partial oxidation of methanol over a Pt/Al_2O_3 catalyst enhanced by sprays. *Energy* **106**, 1–12.

Cheng, K.-Y., Hsieh, L.-L., Yao, K.-S., Lin, C.-H., Chang, E.-J. & Chang, C.-Y. 2010 Decomposition of wastewater containing isopropyl alcohol using the gamma-ray/hydrogen peroxide process. *Environmental Engineering and Management Journal* **20** (3), 151–156.

Eskicioglu, C., Prorot, A., Marin, J., Droste, R. L. & Kennedy, K. J. 2008 Synergetic pretreatment of sewage sludge by microwave irradiation in presence of H_2O_2 for enhanced anaerobic digestion. *Water Research* **42** (18), 4674–4682.

Gao, L., Jiang, Z. & Zhou, J. 2016 Microwave catalyzed oxidative degradation of methyl orange in simulated wastewater using microwave catalytic TiO_2/AC and mechanistic studies. *Current Microwave Chemistry* **3** (1), 38–46.

Hamid, G. A. 2015 Microwave digestion. *Education*. https://www.slideshare.net/GamalAbdulHamid/microwave-digestion

Haque, S., Khan, S., Wahid, M., Dar, S. A., Soni, N., Mandal, R. K., Singh, V., Tiwari, D., Lohani, M., Areeshi, M. Y., Govender, T., Kruger, H. G. & Jawed, A. 2016 Artificial intelligence vs. statistical modeling and optimization of continuous bead milling process for bacterial cell lysis. *Frontiers in Microbiology* **7**, 1852.

Iboukhoulef, H., Amrane, A. & Kadi, H. 2013 Microwave-enhanced Fenton-like system, $Cu(II)/H_2O_2$, for olive mill wastewater treatment. *Environmental Technology* **34** (7), 853–860.

Ivanescu, A. E., Li, P., George, B., Brown, A. W., Keith, S. W., Raju, D. & Allison, D. B. 2016 The importance of prediction model validation and assessment in obesity and nutrition research. *International Journal of Obesity (London)* **40** (6), 887–894.

Jou, C. J. 2008 Degradation of pentachlorophenol with zero-valence iron coupled with microwave energy. *Journal of Hazardous Materials* **152** (2), 699–702.

Körbahti, B. K. 2007 Response surface optimization of electrochemical treatment of textile dye wastewater. *Journal of Hazardous Materials* **145** (1), 277–286.

Kuila, S. B. & Ray, S. K. 2013 Separation of isopropyl alcohol–water mixtures by pervaporation using copolymer membrane: analysis of sorption and permeation. *Chemical Engineering Research and Design* **91** (2), 377–388.

Lai, T.-L., Lee, C.-C., Wu, K.-S., Shu, Y.-Y. & Wang, C.-B. 2006 Microwave-enhanced catalytic degradation of phenol over nickel oxide. *Applied Catalysis B: Environmental* **68** (3), 147–153.

Lee, C. L., Lin, C. & Jou, C. J. 2012 Microwave-induced nanoscale zero-valent iron degradation of perchloroethylene and pentachlorophenol. *Journal of the Air Waste Management Association* **62** (12), 1443–1448.

Lin, S. H. & Wang, C. S. 2004 Recovery of isopropyl alcohol from waste solvent of a semiconductor plant. *Journal of Hazardous Materials* **106** (2), 161–168.

Liu, X., An, S., Shi, W., Yang, Q. & Zhang, L. 2014 Microwave-induced catalytic oxidation of malachite green under magnetic Cu-ferrites: new insight into the degradation mechanism and pathway. *Journal of Molecular Catalysis A: Chemical* **395**, 243–250.

Liu, Z., Meng, H., Zhang, H., Cao, J., Zhou, K. & Lian, J. 2018 Highly efficient degradation of phenol wastewater by microwave induced H_2O_2-CuOx/GAC catalytic oxidation process. *Separation and Purification Technology* **193**, 49–57.

Menéndez, J. A., Arenillas, A., Fidalgo, B., Fernandez Diez, Y., Zubizarreta, L., Calvo, E. G. & Bermúdez, J. M. 2010 Microwave heating processes involving carbon materials. *Fuel Processing Technology* **91**, 1–8.

Mohammadi, L., Bazrafshan, E., Noroozifar, M., Ansari-Moghaddama, A. R., Khazaei Feizabad, A. R. & Mahvi, A. H. 2017 Optimization of the catalytic ozonation process using copper oxide nanoparticles for the removal of benzene from aqueous solutions. *Global Journal of Environmental Science and Management* **3** (4), 403–416.

Mohanraj, P., Prasanna, S. & Miranda, L. R. 2015 Phenol degradation using microwave irradiation. *Journal of Chemical and Pharmaceutical Research* **7** (3), 111–117.

Montgomery, D. 2014 *Design and Analysis of Experiments*. John Wiley and Sons, New York, USA.

Parolin, F., Nascimento, U. M. & Azevedo, E. B. 2013 Microwave-enhanced UV/H_2O_2 degradation of an azo dye (tartrazine): optimization, colour removal, mineralization and ecotoxicity. *Environmental Technology* **34** (10), 1247–1253.

Polaert, I., Estel, L. & Ledoux, A. 2005 Microwave-assisted remediation of phenol wastewater on activated charcoal. *Chemical Engineering Science* **60** (22), 6354–6359.

Prasannakumar Beri, R., Regupathi, I. & Murugesan, T. 2008 An optimization study on microwave irradiated decomposition of phenol in the presence of H_2O_2. *Journal of Chemical Technology & Biotechnology* **84** (1), 83–91.

Quan, X., Zhang, Y., Chen, S., Zhao, Y. & Yang, F. 2007 Generation of hydroxyl radical in aqueous solution by microwave energy using activated carbon as catalyst and its potential in removal of persistent organic substances. *Journal of Molecular Catalysis A: Chemical* **263** (1), 216–222.

Regulska, E., Brus, D. M., Rodziewicz, P., Sawicka, S. & Karpinska, J. 2016 Photocatalytic degradation of hazardous Food Yellow 13 in TiO_2 and ZnO aqueous and river water suspensions. *Catalysis Today* **266**, 72–81.

Remya, N. & Lin, J.-G. 2011 Current status of microwave application in wastewater treatment – a review. *Chemical Engineering Journal* **166** (3), 797–813.

Sarrai, A. E., Hanini, S., Merzouk, N. K., Tassalit, D., Szabó, T., Hernádi, K. & Nagy, L. 2016 Using central composite experimental design to optimize the degradation of tylosin from aqueous solution by photo-Fenton reaction. *Materials* **9** (6), 428.

Singh, C., Chaudhary, R. & Gandhi, K. 2013 Preliminary study on optimization of pH, oxidant and catalyst dose for high COD content: solar parabolic trough collector. *Iranian Journal of Environmental Health Science & Engineering* **10** (1), 13.

Sivilotti, M. L. A. 2019 Isopropyl alcohol poisoning. https://www.uptodate.com/contents/isopropyl-alcohol-poisoning.

Wikipedia Student's t-test, https://en.wikipedia.org/wiki/Student%27s_t-test

Xiao, Y., Xu, H.-Y., Xie, H.-M., Yang, Z.-H. & Zeng, G.-M. 2015 Comparison of the treatment for isopropyl alcohol wastewater from silicon solar cell industry using SBR and SBBR. *International Journal of Environmental Science and Technology* **12**, 2381–2388.

Xu, D., Cheng, F., Lu, Q. & Dai, P. 2014 Microwave enhanced catalytic degradation of methyl orange in aqueous solution over CuO/CeO_2 catalyst in the absence and presence of H_2O_2. *Industrial & Engineering Chemistry Research* **53** (7), 2625–2632.

Yang, S., Xu, Y., Huang, Y., Zhou, G., Yang, Z., Yang, Y. & Wang, G. 2013 Photocatalytic degradation of methyl violet with $TiSiW_{12}O_{40}/TiO_2$. *International Journal of Photoenergy* 1–5.

Yin, J., Cai, J., Yin, C., Gao, L. & Zhou, J. 2016 Degradation performance of crystal violet over CuO@AC and CeO_2-CuO@AC catalysts using microwave catalytic oxidation degradation method. *Journal of Environmental Chemical Engineering* **4** (1), 958–964.

Younis, S., El-azab, W., El-Gendy, N., Qarani Aziz, S., Moustafa, Y. M. M., Aziz, H. A. & Abu Amr, S. 2014 Application of response surface methodology to enhance phenol removal from refinery wastewater by microwave process. *International Journal of Microwave Science and Technology* 1–14.

Zhang, A. & Li, Y. 2014 Removal of phenolic endocrine disrupting compounds from waste activated sludge using UV, H_2O_2, and UV/H_2O_2 oxidation processes: effects of reaction conditions and sludge matrix. *Science of the Total Environment* **493**, 307–323.

Zhang, Z., Shan, Y., Wang, J., Ling, H., Zang, S., Gao, W., Zhao, Z. & Zhang, H. 2007 Investigation on the rapid degradation of Congo red catalyzed by activated carbon powder under microwave irradiation. *Journal of Hazardous Materials* **147** (1), 325–333.

Zhang, Z., Xu, Y., Ma, X., Li, F., Liu, D., Chen, Z., Zhang, F. & Dionysiou, D. D. 2012 Microwave degradation of methyl orange dye in aqueous solution in the presence of nano-TiO_2-supported activated carbon (supported-TiO_2/AC/MW). *Journal of Hazardous Materials* **209–210**, 271–277.

Zhang, Z., Jiatieli, J., Liu, D., Yu, F., Xue, S., Gao, W., Li, Y. & Dionysiou, D. D. 2013 Microwave induced degradation of parathion in the presence of supported anatase- and rutile-TiO_2/AC and comparison of their catalytic activity. *Chemical Engineering Journal* **231**, 84–93.